

UAV-BS-based Hybrid OMA-NOMA System with Multiple Antennas for Multi-user Communication

Ameer Y. Sadeeq and Mohamad A. Ahmed

Ninevah University, Mosul, Iraq

<https://doi.org/10.26636/jtit.2025.2.2045>

Abstract — In this paper, an unmanned aerial vehicle (UAV) using hybrid orthogonal multiple access (OMA) and non-orthogonal multiple access (NOMA) solutions aided by multiple input multiple output (MIMO) technology is proposed to provide wireless communication for ground users (GUs). The proposed OMA-NOMA-MIMO system aims to improve throughput and spectrum efficiency. Additionally, it also strives to maximize the sum rate while achieving good user fairness. UAVs are considered as base stations (BSs) that provide services to users in multiple real-life scenarios, e.g. during natural disasters. They also enable aerial surveillance and help establish BSs during mass events. A pairing algorithm is proposed for far-near NOMA users with an optimized power allocation (PA) mechanism to improve the performance of NOMA-UAV-BS. Channels between UAV-BS and GU are established as being of the line-of-sight (LoS) and non-line-of-sight (NLoS) varieties, taking into consideration the angle of departure (AoD) and the angle of arrival (AoA). The results obtained demonstrate that NOMA performs best in specific scenarios, while OMA overcomes NOMA in others. The outcomes of the project may be utilized to control the transmission performed by the UAV-BS by serving the GUs depending on the required quality of service.

Keywords — *non-orthogonal multiple access, pairing algorithms, successive interference cancellation, unmanned aerial vehicle*

1. Introduction

Unmanned aerial vehicles (UAVs) may be useful in providing access to wireless networks by acting as base stations (BS) to expand coverage at a location where a fixed radio BS is not available [1]– [3]. Commonly, in wireless cellular communication, such as 2G, 3G, and 4G systems that rely on orthogonal multiple access (OMA) techniques in the air interface, each user is assigned a single resource block, enjoys limited throughput, and suffers from insufficient user fairness [4], [5]. The problem becomes more acute when the number of users increases in congested areas.

The non-orthogonal multiple access (NOMA) technique is designed for 5G and beyond radio access cellular networks. This multiple access solution is capable of simultaneously utilizing a single resource block, i.e. the same frequency band, for several users. This mechanism leads to a significant improvement in throughput and spectrum efficiency, with satisfactory user fairness levels. Therefore, in this article, the

focus will be on using NOMA for UAV-BS to overcome the challenges faced by OMA radio access technologies [3], [6]. Serving multiple users in NOMA can be achieved by assigning a different power level to each user. On the contrary, serving users in OMA is implemented by assigning a fixed power level for each user. This primary difference leads to OMA outperforming NOMA in terms of spectral efficiency and throughput [7], [8]. To further enhance NOMA's performance, multiple input multiple output (MIMO) technology may be merged with NOMA, as suggested in [8], [9].

In this paper, a pairing algorithm is proposed for the NOMA technology which divides the multiple users into groups, i.e., clusters, with each group consisting of two users. In other words, the mechanism pairs a user with a good channel gain (stronger user) with another user with poor channel gain (weak user) [10]. The channel proposed between UAV-BS and the ground user (GU) is, in some cases, of the line of sight (LoS) and in other cases of the non-LoS (NLoS) variety, taking into consideration the probability of LoS and NLoS [11]. We assume that the superimposed NOMA signal from UAV-BS reaches GU over a Rician fading channel.

Some key parameters play an important role in determining the quality of the channel. These include the following: Rician factor, path loss exponent, distance between UAV-BS and GU, angle of departure (AoD), angle of arrival (AoA) and carrier wavelength [12].

The authors contribution to previous works is summarized as follows:

- In this work, we investigate unmanned aerial vehicles (UAV) relying on hybrid orthogonal multiple access (OMA) and nonorthogonal multiple access (NOMA) mechanisms, aided by the multiple input multiple output (MIMO) technology. Several metrics have been measured at different GUs using two channel types (LoS and NLoS) to estimate the sum rate GU with the overall rate of NOMA and OMA and determine the probability of P_{out} outage, with a comparison between NOMA and OMA.
- To enhance the overall performance of the system, UAV-BSs are equipped with the MIMO technology.
- The pairing algorithm is employed to significantly improve spectral efficiency and achieve better user fairness. All users who are underserved by the UAV-BS are divided

into multiple groups according to such parameters as user channel gain (weak or strong), user data rate, and distance of the user from the UAV-BS.

- To account for all potential channels that may be established between the UAV-BS and GU, we consider LoS and NLoS channels. To make the channel calculations more accurate, we consider the elevation and azimuth of AoD and AoA along with Rician fading and Rayleigh fading.
- In [13], non-linear energy harvesting in NOMA systems with a fixed base station has been proposed and investigated, while in this work, we propose a hybrid OMA-NOMA scheme intended specifically for UAV-based BSs equipped with MIMO antennas to serve multiple users in no coverage areas.
- In [14], the SIC error on near and far users in the NOMA technology is studied by estimating the near- and far-user BER. The outcomes prove the superiority of NOMA over OMA. Here, we estimated P_{out} and sum rate for each user in NOMA and OMA and we used SIC without the error effect on near and far users in NOMA.
- In [15], different antenna techniques are developed to improve the performance of wireless mobile communication using the MIMO technology. Our study models UAV-BS MIMO communication with explicit AoD and AoA considerations under Rician fading, thus ensuring more accurate channel estimation for aerial systems.

The rest of the paper is arranged as follows. A model of the system is presented in Section 2, and the pairing of users is described in Section 3. Section 4 outlines the detection process performed by the receiver. Simulation results and discussions are presented in Section 5, with conclusions contained in Section 6.

2. System Model

As illustrated in Fig. 1, we propose that several users, i.e. $U_1, U_2, U_3, \dots, U_N$ present at a particular location take advantage of the services provided by a UAV-BS by applying either the NOMA or OMA technology. It is assumed that the users are located at different distances, i.e. $d_1, d_2, d_3, \dots, d_N$, from the UAV. According to these distances, U_1 is the weakest user due to being located at the furthest distance from the base station (UAV) (this user has a poor channel gain). U_4 is the strongest user due to being located the closest (strong channel gain) to the UAV.

According to the principles of NOMA, the power allocation coefficients for each user are denoted by $a_1, a_2, a_3, \dots, a_N$. The larger portion of the power is assigned to the weakest users (farthest), while a lower power level is assigned to the strongest users (nearest) to ensure user fairness [3]. The combined power allocation coefficients provided by the UAV-BS should equal 1, in accordance with the NOMA theory [16].

The UAV-BS is equipped with multiple antennas N_t , while each GU is equipped with antenna N_r . Such a MIMO structure

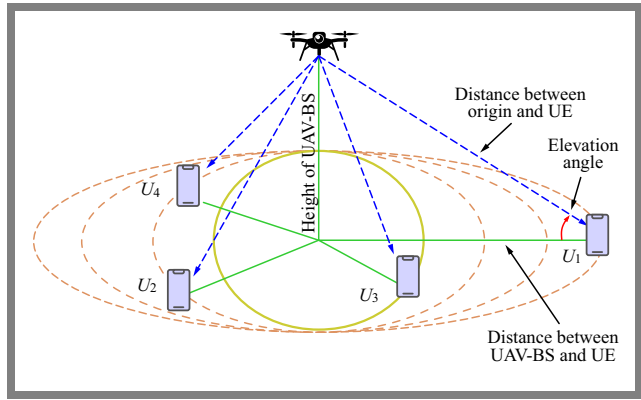


Fig. 1. Model of a UAV-BS communication system.

is intended to enhance the performance of the proposed NOMA system [16].

Three NOMA power allocation schemes may be used for UAV-based wireless communication: fixed power allocation (FPA), equal power allocation (EPA) and fractional transmit power allocation (FTPA) [3], [17].

- In FPA: the distance between the user and the UAV-BS is taken into consideration; low power is allocated to a given user if it is located close to the UAV base station, and vice versa.
- In EPA: constant power is allocated to all users and the distance between the user and the UAV-BS is also taken into consideration (a distinction is made whether the user is close to or far away from the UAV base station).
- In FTPA: the power is allocated dynamically, meaning that the distance between the user and the UAV-BS is taken into consideration. In other words, FTPA allocates low power to users who enjoy good channel conditions and high power to users with poor channel conditions. This approach ensures fairness between users in terms of power allocation [3].

Several scenarios are considered to evaluate the GUs rates, the UAV-BS's sum rate, error probability (bit error rate – BER), and spectral efficiency (SE) for the proposed system by relying on orthogonal multiple access (OMA) and NOMA techniques under different channels conditions.

In the first scenario, we assume that U_1 is the user located the farthest from the UAV-BS. The highest power allocation coefficient is assigned to this user, considering a_2, a_3, \dots, a_N as interference. The achievable rate at the n -th user is [3]:

$$R_1 = B \log_2 \left(1 + \frac{a_1 p_t g_1}{a_2 p_t g_1 + a_3 p_t g_1 + a_4 p_t g_1 + w_1} \right), \quad (1)$$

where p_t is the transmit power of the UAV-BS, and for any n -th user, power allocation factor (PAF), noise power and channel gain are denoted by a_n, w_n , and g_n , respectively.

At the second user, U_2 , PAF is lower than the one assigned to U_1 , as the user has better channel gain, i.e. ($a_1 > a_2$), and this mechanism is applied to the rest of the users depending on their channel gain, i.e. ($a_1 > a_2 > a_3 > a_4$). Furthermore, all users, except the farthest one, require the application of SIC to subtract the superposed signals of higher order users.

Therefore, the achievable rate at U_2 after removing the signal of U_1 is given as:

$$R_2 = B \log_2 \left(1 + \frac{a_2 p_t g_2}{a_3 p_t g_2 + a_4 p_t g_2 + w_2} \right). \quad (2)$$

For the third user, the achievable rate at U_3 , after removing interference caused by the signals of U_1 and U_2 , is given as:

$$R_3 = B \log_2 \left(1 + \frac{a_3 p_t g_3}{a_4 p_t g_3 + w_3} \right). \quad (3)$$

The same procedure is applied to the fourth user, in which case the achievable rate at U_4 , after applying SIC to remove all interfering signals caused by other users with higher PAFs, is expressed as:

$$R_4 = B \log_2 \left(1 + \frac{a_4 p_t g_4}{w_4} \right). \quad (4)$$

On the other hand, when the OMA technique is used, instead of NOMA, to serve the same four users, the achievable rates for any user can be given as:

$$R_n^{OMA} = 0.5 B \log_2 \left(1 + \frac{p_t g_n}{w_n} \right). \quad (5)$$

The average rate for a particular user served by NOMA, i.e. the n -th user, is:

$$\bar{R}_n = E\{R_n\}, \quad (6)$$

where $E\{\cdot\}$ refers to the expectation process.

Similarly, the average rate achievable by any user served by OMA can be expressed as [18]:

$$\bar{R}_n^{OMA} = E\{R_n^{OMA}\}. \quad (7)$$

The sum rate SR of the NOMA system, i.e., the overall rate provided by the UAV, can be found by adding the individual rates of all users:

$$SR_{NOMA} = \sum_{n=1}^N R_n. \quad (8)$$

The sum rate of the OMA system can be determined by adding up the individual rates of users:

$$SR_{OMA} = \sum_{n=1}^N R_n^{OMA}. \quad (9)$$

Furthermore, spectral efficiency SE , in bits/sec/Hz, regardless of the technique used, is:

$$SE = \frac{SR}{BW}. \quad (10)$$

2.1. Channel Model

As shown in Fig. 2, the channels between the GUs and UAV-BS are of the LoS and NLoS variety [19]. These channels are impacted by environmental factors prevailing within the coverage area, represented by the density and altitude of the buildings as well as the distance between the ground and the UAV-BS [11].

The total path loss, as shown in Fig. 2, of both GUs in cluster 1, i.e. U_1 and U_2 , is computed either directly, based on the free-space path loss, or based on the excessive losses that occurred

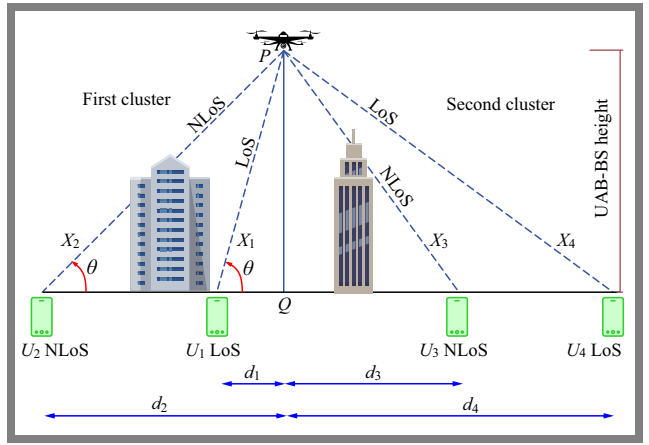


Fig. 2. Channel model with LoS and NLoS links, where $\{X_1, X_2, X_3, X_4\}$ represent the actual physical distances between the GUs and the UAV-BS.

Tab. 1. Path loss exponent for different environments [20].

Type of environment	η
Free space	2
Urban area cellular radio	2.7 to 3.5
Shadowed urban cellular radio	3 to 5
In building line-of-sight	1.6 to 1.8
Obstructed by buildings	4 to 6
Obstructed by factories	2 to 3

along the NLoS paths due to reflections of the transmitted signals from obstacles within the coverage area.

The power received by j -th user is determined as in [11]:

$$Prx_j(\text{dB}) = Ptx(\text{dB}) - L_j(\text{dB}). \quad (11)$$

where Ptx indicates the power transmitted by the UAV-BS and L_j indicates the path loss of the air-to-ground (A2G) channel between the UAV-BS and any GU. The path loss for the A2G channel for the j -th link is represented by distance X_j and is evaluated similarly to [11] for LoS and NLoS links, as:

$$L_j = 10 \eta \log_{10}(X_j) + X_{LoS}, \quad (12)$$

$$L_j = 10 \eta \log_{10}(X_j) + X_{NLoS}, \quad (13)$$

respectively, where η represents the path loss exponent, which is considered one of the important parameters in wireless communication. The value of the loss-pass exponent is affected by environmental factors, such as interference, reflection, and diffraction. The value of the path loss exponent for different environments is presented in Tab. 1. In addition, X_{LoS} and X_{NLoS} represent the excessive path losses of both LoS and NLoS links, respectively.

The probability that a GU has a LoS link with a UAV-BS is given by [11]:

$$Pr_{LoS}(j) = \frac{1}{1 + \alpha e^{-\beta(\theta_j - \alpha)}}, \quad (14)$$

Tab. 2. α and β values of various environment types [3].

Environment	α	β
Suburban	0.1	750
Urban	0.3	500
Dense urban	0.5	300
Urban high-rise	0.5	300

where α and β are constant values linked to a given environmental profile, such as urban area, dense urban area, etc. The range of α and β varies from 0.1 to 0.8 and 100 to 750, respectively. In practical terms, α is the ratio of the ground area covered by buildings to the total ground area (dimensionless) and β is the number of buildings per square kilometer [3].

In Tab. 2, some examples of α and β values for various environment types are presented.

The probability of a ground user having an NLoS link with a UAV-BS is given by [11]:

$$Prj(NLoS) = 1 - Prj(LoS). \quad (15)$$

In general, the UAV is not aware of the type of terrain in its vicinity to specify the type of link (LoS or NLoS). Therefore, Eq. (12) is reworked as [11]:

$$Prx, j \text{ (dB)} = Ptx \text{ (dB)} - \bar{L}_j(Rc, H). \quad (16)$$

where $\bar{L}_j(Rc, H)$ determines the mean path loss including probabilities for a LoS and NLoS link between the UAV-BS and ground user. It is calculated as follows [11]:

$$\bar{L}_j(Rc, H) = Prj(LoS)L_j(LoS) + Prj(NLoS)L_j(NLoS). \quad (17)$$

As mentioned above, the signal from the UAV-BS reaches the GU directly by LoS and not directly by NLoS over the Rician fading channel. In this paper, we considered both AoD and AoA cases.

The channel between the UAV-BS and the ground user with LoS and NLoS is expressed as follows [12]:

$$H = \sqrt{\xi \frac{K}{K+1}} b(\theta_x, \theta_y)_{AoA} a(\theta_x, \theta_y)_{AoD} + \sqrt{\frac{\xi}{K+1}} \bar{H}. \quad (18)$$

where \bar{H} is the NLoS component, $\xi = d^{-\eta}$ represents large-scale fading, K is the Rician factor, while a and b are the steering vectors of the UAV-BS and the ground user, respectively.

The Rician factor K represents the ratio between the power of the LoS component and the power of the scattered (NLoS) [21], i.e., it is the parameter representing the strength of the LoS component:

$$K = \frac{P_{LoS}}{P_{NLoS}}. \quad (19)$$

This factor measures fading severity, for example $K = 0$ represents NLoS (Rayleigh channel), and $K = \infty$ represents LoS (absent fading case). In other words, when $K \gg 1$, strong LoS dominance is present. The different values of the Rician factor for various environments are shown in Tab. 3.

Tab. 3. Rician factor K for different environments [18].

Environment	Rician K factor [dB]
Lake	13.10
Hilly	13.61
Rural	9.28
Suburban	6.93

On the UAV-BS side, the elevation and azimuth (AoD) along x and y axes are as follows [12]:

$$\theta_{xAoD} = -\frac{2\pi d_{BS}}{\lambda} \cos \theta_{BS} \cos \phi_{BS}, \quad (20)$$

$$\theta_{yAoD} = -\frac{2\pi d_{BS}}{\lambda} \cos \theta_{BS} \sin \phi_{BS}. \quad (21)$$

On the GU side, the elevation and azimuth (AoA) along x and y axes are [12]:

$$\theta_{xAoA} = \frac{2\pi d_{GU}}{\lambda} \cos \theta_{GU} \cos \phi_{GU}, \quad (22)$$

$$\theta_{yAoA} = \frac{2\pi d_{GU}}{\lambda} \cos \theta_{GU} \sin \phi_{GU}. \quad (23)$$

Channel gain is:

$$g_n = |H_n * w_n|^2, \quad (24)$$

where H_n and w_n are the channel matrix and the beamforming vector for the n -th user, respectively.

Beamforming techniques can be employed in wireless communications systems to eliminate inter-user interference. One of the most powerful and efficient approaches is the zero-force (ZF) beamforming method. It is considered a linear beamforming precoder that applies weight to users' signals at the UAV-BS in the downlink phase of the transmission. The ZF precoding vector for the n -th user that passes through channel H_n can be expressed as:

$$w_n = \rho H_n^H (H_k H_n^H)^{-1}, \quad (25)$$

with

$$\rho = \frac{1}{\sqrt{Tr(H H^H)^{-1}}}, \quad (26)$$

where ρ is a normalization value that satisfies transmitting signals within the available transmitted power of the UAV-BS. Furthermore, $(A)^{-1}$, $Tr(A)$, and A^H are used to denote the operations of matrix inversion, a trace of a matrix, and the Hermitian transport of matrix A , respectively.

3. Pairing Users

The pairing algorithm is used to improve spectral efficiency and achieve better user fairness for systems utilizing the NOMA technique with many users. By using the pairing technique, the system obtains the required information about the users' circumstances, i.e. the channel gain, and utilizes this information for dividing the coverage area into clusters, with each of them comprising a specific number of users. The pairing algorithm plays a significant role in selecting users with different channel gains to be served by the UAV-BS. In

each cluster, a high power level is allocated to the user who has a weak channel gain, i.e., the far user (FU), while a lower power level is allocated to a user who has a strong channel gain, i.e., the near user (NU) [13]. Figure 3 shows the paired users within clusters and the SIC operation associated with NOMA, relied upon to detect the signal for each user from the superposed NOMA signal.

In this paper, we consider all users within the coverage area of the UAV-BS, divided into groups based on a pairing algorithm. Each group M is to serve $2M$ users, meaning each cluster contains two paired users. The pairing algorithms perform tests to arrange channel gains g_n of all users in a descending order, i.e., $g_1 \geq g_2 \geq \dots \geq g_{2M}$. The UAV-BS establishes the first group by pairing the nearest user characterized by channel gain g_1 with the farthest user having channel gain g_{2M} . Then, the second user in the list g_2 is paired with users g_{2M-1} . This operation is continued in the same manner until all users are paired within their clusters.

It is worth noting that this way of pairing is called near-far pairing (NF) [10]. Algorithm 1 shows the NF pairing algorithm for NOMA technology users [21], [22].

Algorithm 1 Near-far (NF) pairing algorithm.

Input: Channel gain for users $g_n = [g_1 + g_2 + \dots + g_{2M}]$, number of groups, number of users $2M$

- 1: Arrange channel gain of all users in downward order:
 $g_1 \geq g_2 \geq \dots \geq g_{2M}$
- 2: Determine the group of channel gains:
 $Q = \{g_1, g_2, \dots, g_{2M}\}$
- 3: **for** $P = 1$ to M **do**
- 4: $g_n = \{ \}$
- 5: $g_{max} = \max\{Q\}, g_{min} = \min\{Q\}$
- 6: $g_n = g_{max} \cup g_{min}$
- 7: $Q = Q(p + 1 : \text{end} - 1)$
- 8: **end for**

Output: Group of pairs

It is noteworthy that their other pairing strategies, such as near-near (NN) pairing and far-far (FF) pairing, which can be used for this purpose, are available as well.

4. Detection Operation

In the receiver, the superimposed NOMA signal from the UAV-BS is received by multiple users. In accordance with the NOMA principle, two users (near and far) are grouped within one cluster with the use of a pairing technique. As mentioned above, a lower PAF is provided to the NU, i.e. the user with strong channel gain, and a high PAF is given to the FU, the one with weak channel gain.

Furthermore, the NU needs the SIC to be implemented to eliminate interference caused by the power of the far user, which is considered significantly high. The SIC process is implemented at the NU terminal by detecting the strong signal of the FU, which is subtracted afterward from the

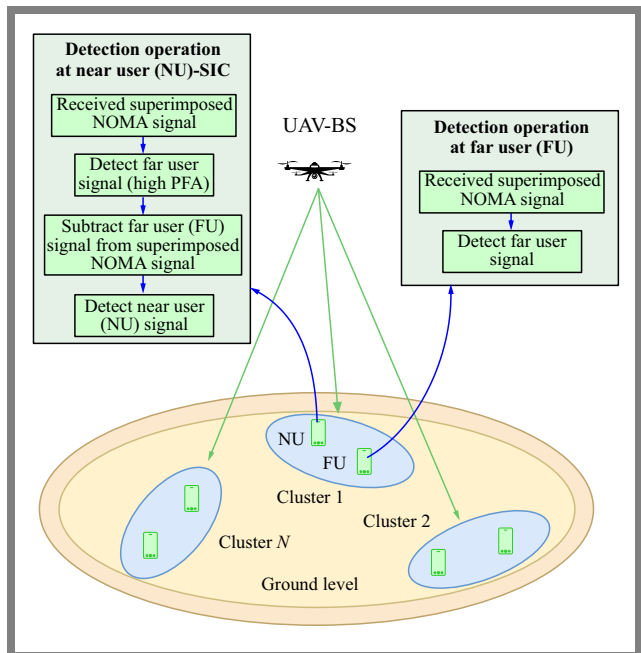


Fig. 3. Detecting the NOMA signal in the NU and FU receivers after the pairing operation.

superimposed NOMA signal to obtain an interference-free signal of the NU [20], [21].

Meanwhile, on the FU side, the detection of the FU signal is realized directly without applying SIC, by considering the interference caused by the NU, which is considered, due to low PAF, to be additive noise. This process for the two users is illustrated in Fig. 3.

5. Simulation Results and Discussions

The simulations described in this paper were conducted using the Matlab programming suite, with the aim of evaluating such performance metrics as the achievable rate and the P_{out} . The performance of the proposed system relying on the NOMA technique is compared with the traditional OMA approach over different scenarios.

In the first scenario, the MIMO-NOMA technology is considered, in which the UAV-BS is equipped with N_t and each user has N_r . We assume that the UAV-BS provides services to users in suburban areas with obstructions in the form of buildings. Therefore, the Rician fading channel between the UAV-BS and GUs is considered with a Rician factor of $K = 6.93$ dB, and the path loss exponent is assumed to be $\eta = 4$. All the parameters used in the simulation are listed in Tab. 4.

In MIMO-NOMA, the pairing algorithm has been applied to choose every two users in one ground. On the GU side, two scenarios need to be considered for detection of the MIMO receiver: in the first case, the NU has a low PAF and it is necessary to apply the SIC operation to remove the interference. The second case, the FU has a high PAF, meaning that no SIC is required. The distances between the UAV-BS and the FU and NU as GUs are $d_F = 300$ and $d_N = 150$, respectively. The power allocation coefficients

Tab. 4. Simulation parameters.

Notation	Parameter	Value
K	Rician K factor	6.93 dB
d_F	Distance between UAV-BS and FU	300 m
d_N	Distance between UAV-BS and NU	150 m
a_F	Power allocation coefficient for FU	0.88
a_N	Power allocation coefficient for NU	0.12
η	Path loss exponent	4
d_λ	Antenna spacing	0.5λ
$N_t \times N_r$	MIMO antenna	$2 \times 2, 8 \times 2$
N_s	Number of transmitted symbols	10^5
(φ, θ) UAV-BS	Azimuth and elevation angles for FU and NU	$(30^\circ, 45^\circ)$ and $(90^\circ, 45^\circ)$
(φ, θ) GU	Azimuth and elevation angles for FU and NU	$(60^\circ, 30^\circ)$ and $(60^\circ, 30^\circ)$
f_o	Operation frequency	410 MHz to 7.125 GHz
BW	Bandwidth	20 MHz
P_t	Transmitted power by UAV-BS	0 – 40 dBm
R_n	The target rate for NU	4 bit/sec/Hz
R_F	The target rate for FU	3 bit/sec/Hz

assigned by the UAV-BS to the FU and NU are $a_F = 0.88$ and $a_N = 0.12$, respectively. In addition, the azimuth and elevation angles equal $\{30^\circ, 45^\circ\}$ and $\{90^\circ, 45^\circ\}$ for the FU and NU, respectively. On the GU side, the azimuth and elevation angles are $\{60^\circ, 30^\circ\}$ and $\{60^\circ, 30^\circ\}$ towards the FU and NU, respectively. The bandwidth is 20 MHz.

The individual data rates for the FU and NU, with MIMO-NOMA and MIMO-OMA deployed at the UAV-BS, are shown in Fig. 4. The two techniques are assumed to provide services to all users under the same conditions, with changes to the number of antennas used by the UAV-BS and the two users. Two scenarios for the MIMO approach for $N_t \times N_r$ as 2×2 and 8×2 are presented. One may notice from this figure that NOMA offers better performance for users with weak channel gains, while OMA is a better choice for users with strong channel gains. Moreover, depending on the data rate required for a specific user within the cluster, the UAV-BS may switch from NOMA to OMA, may rely on a hybrid NOMA-OMA approach or make the required changes on the PAFs of the NOMA system to improve the rate of a particular user. It can also be noticed that increasing the number of antennas at the UAV-BS may significantly improve the rate for all users.

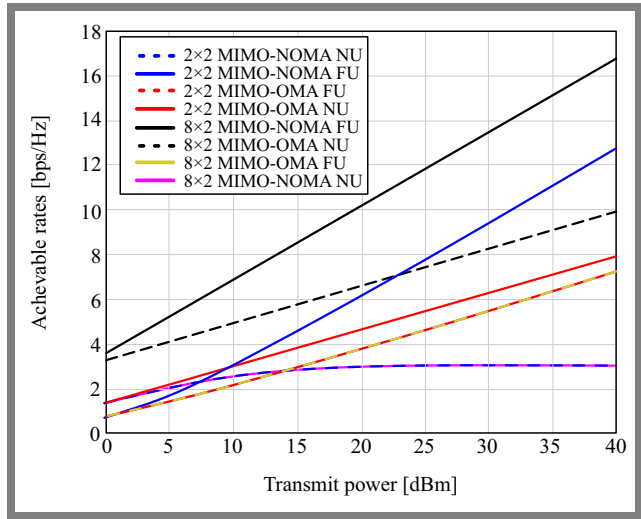
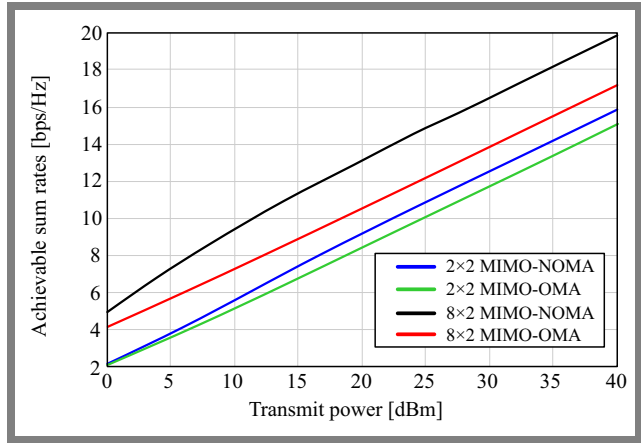

Fig. 4. Individual data rates of two users with NOMA and OMA applied for different numbers of N_t and N_r .

Fig. 5. Sum rates of NOMA and OMA technologies with different numbers of N_t and N_r .

Figure 5 shows the sum rates for the proposed system under the same conditions mentioned above and for different numbers of N_t and N_r . The transmitted power of the UAV-BS is 40 dBm. NOMA outperforms OMA with approximately 3 bps/Hz and 0.7 bps/Hz for N_t being equal to 8 and 2, respectively, and for a fixed $N_r = 2$.

Figure 6 shows the P_{out} for the proposed NOMA and OMA systems. The P_{out} represents the probability that a user obtains a data rate R that is below the target rate required for an acceptable quality of service (QoS). For this simulation, the required rate for the NU was $R_n = 4$ bps and the FU was $R_f = 3$ bps.

One may notice that a lower P_{out} may be obtained in the FU's receiver in the case of 8×2 MIMO-NOMA, since this user has been allocated a higher PAF to overcome its weak channel gain. The second and third best P_{out} occurred for the cases of 8×2 MIMO-OMA in the NU and FU, respectively, due to the entire available power being served to these users by OMA.

On the other hand, the worst P_{out} is obtained for the cases of 2×2 MIMO-NOMA and 8×2 MIMO-NOMA at the NU

Tab. 5. Comparison of results obtained with outcomes of related works, for 35 dBm.

Ref.	BS type	No. of users	Path-loss exponent	MIMO ($N_t \times N_r$)	Sum data rate users [bps/Hz]		Data rate NOMA [bps/Hz]		Data rate OMA [bps/Hz]		P_{out} NOMA $\times 10^{-6}$		P_{out} OMA $\times 10^{-6}$	
					NOMA	OMA	FU	NU	FU	NU	FU	NU	FU	NU
[18]	Fixed ground BS	4	4	SISO	15.8	NA	NA	NA	NA	NA	NA	NA	NA	NA
				2×2	18	NA	8.2	9.5	NA	NA	7943	1584	NA	NA
[24]	Fixed ground BS	2	4	2×1	NA	NA	0.5	2.6	0.4	2.2	31	50	158	251
[25]	UAV-RIS	2	3	NA	NA	NA	NA	NA	NA	NA	1	1	1	1
[26]	Fixed ground BS	2	NA	3×3	5.9	3.9	NA	NA	NA	NA	NA	NA	NA	NA
		3			3.7	3	NA	NA	NA	NA	NA	NA	NA	NA
[27]	Fixed ground BS	2	Not specified	Not specified	NA	NA	2.2	13.8	NA	NA	1584	125	NA	NA
[22]	Fixed ground BS	2	Not specified	2×2	6.1	NA	1.7	10.4	NA	NA	1000	1259	NA	NA
This work	UAV-BS	2	4	2×10	NA	NA	NA	NA	NA	NA	200	251	NA	NA
				2×2	14.152	13.36	12.9	3	7	7.9	39	6309	125	0
				2×8	18.163	15.47	16.9	3	7	9.9	0	2000	0	0

terminal, due to the lower PAF applied to these two scenarios. Additionally, increasing the number of antennas in the UAV-BS can significantly reduce the P_{out} .

As shown in Tab. 5, the proposed UAV-BS system demonstrates superior performance compared to solutions described in previous works, both in fixed ground BSs and UAV-RIS configurations. At 35 dBm, it achieves significantly higher sum data rates and lower outage probabilities. In the case of a 2×8 MIMO configuration, the system reaches a NOMA sum data rate of 18.163 bps/Hz and an OMA sum data rate of 15.47 bps/Hz, outperforming traditional setups. Individual user data rates are also enhanced, particularly in the case of NOMA, where the UAV-BS achieves a result of up to 16.9 bps/Hz for the far user. Furthermore, the proposed system shows a notable reduction in outage probability, reaching zero for both NOMA FU and FU-NU OMA, highlighting improved reliability of the link. These results confirm that UAV-BS systems with large MIMO arrays and beamforming are capable of greatly enhancing network capacity and reliability levels for future wireless communication solutions.

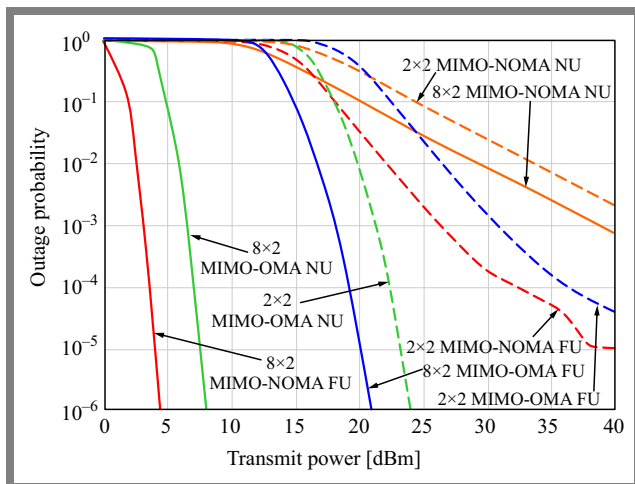


Fig. 6. Outage probabilities for FU and NU after applying NOMA and OMA techniques and utilizing different numbers of antennas.

6. Conclusions

In this paper, a UAV-BS equipped with multiple antennas has been proposed to serve multiple users. The hybrid OMA-NOMA technique is assumed to provide services to all users in the UAV-BS coverage area. Users with strong and weak channel gains are assigned to the same clusters by near-far pairing algorithms.

The UAV-BS provides services by applying the OMA technique between clusters, while the NOMA approach has been applied to users in each cluster by superimposing their signal after allocating each one of them with a suitable PAF. Different scenarios involving channels between the UAV-BS and the GUs have been considered, depending on whether LoS component of the wave existed or not. AoD and AoA angles for all terminals within this system have been given consideration as well.

The results showed that NOMA outperformed OMA in the cluster under some conditions, depending on the choice of suitable PAF levels for the paired users. In addition, OMA demonstrated good performance in terms of P_{out} and throughput when compared with NOMA for strong channel gain users. because of lower PAF levels assigned to these users. Furthermore, the UAV-BS can apply a hybrid mechanism by switching from OMA to NOMA, or the other way round, depending on specific situations and circumstances (i.e. depending on the target throughput and P_{out}).

For future work, several promising projects are envisaged, such as tracking users by the UAV-BS to enhance the performance of the entire system or optimizing the power level by automatically selecting PAF for each user depending on their status. The use of the mmWave technology may be considered as well to boost the overall capacity of the system. Additionally, mechanisms switching between NOMA and OMA may be developed to avoid service interruptions when one of the techniques remains unavailable.

References

- [1] S. Hayat, E. Yanmaz, and R. Muzaffar, "Survey on Unmanned Aerial Vehicle Networks for Civil Applications: A Communications Viewpoint", *IEEE Communications Surveys & Tutorials*, vol. 18, pp. 2624–2661, 2016 (<https://doi.org/10.1109/COMST.2016.2560343>).
- [2] N.R. Zema, E. Natalizio, and E. Yanmaz, "An Unmanned Aerial Vehicle Network for Sport Event Filming with Communication Constraints", *First International Balkan Conference on Communications and Networking (Balkancom 2017)*, Tirana, Albania, 2017.
- [3] L.M. Mei, M.S. Johal, F. Idris, and N. Hashim, "Spectrally Efficient UAV Communications Using Non-orthogonal Multiple Access (NOMA)", *Journal of Advanced Research in Applied Sciences and Engineering Technology*, vol. 43, pp. 227–242, 2025 (<https://doi.org/10.37934/araset.43.1.227242>).
- [4] J. Ghosh *et al.*, "Performance Investigation of NOMA versus OMA Techniques for mmWave Massive MIMO Communications", *IEEE Access*, vol. 9, pp. 125300–125308, 2021 (<https://doi.org/10.1109/ACCESS.2021.3102301>).
- [5] W. Jaafar *et al.*, "Multiple Access in Aerial Networks: From Orthogonal and Non-orthogonal to Rate-splitting", *IEEE Open Journal of Vehicular Technology*, vol. 1, pp. 372–392, 2020 (<https://doi.org/10.1109/OJVT.2020.3032844>).
- [6] S.K. Zaidi *et al.*, "Exploiting UAV as NOMA Based Relay for Coverage Extension", *2019 2nd International Conference on Computer Applications & Information Security (ICCAIS)*, Riyadh, Saudi Arabia, 2019 (<https://doi.org/10.1109/CAIS.2019.8769542>).
- [7] A. Li, Y. Lan, X. Chen, and H. Jiang, "Non-orthogonal Multiple Access (NOMA) for Future Downlink Radio Access of 5G", *China Communications*, vol. 12, pp. 28–37, 2015 (<https://doi.org/10.1109/CC.2015.7386168>).
- [8] G. Liu *et al.*, "Hybrid Half-duplex/full-duplex Cooperative Non-orthogonal Multiple Access with Transmit Power Adaptation", *IEEE Transactions on Wireless Communications*, vol. 17, pp. 506–519, 2017 (<https://doi.org/10.1109/TWC.2017.2767601>).
- [9] K. Higuchi and Y. Kishiyama, "Non-orthogonal Access with Random Beamforming and Intra-beam SIC for Cellular MIMO Downlink", *2013 IEEE 78th Vehicular Technology Conference (VTC Fall)*, Las Vegas, USA, 2013 (<https://doi.org/10.1109/VTCFall.2013.6692307>).
- [10] A. Abd Saeed and M.A. Ahmed, "Cognitive Radio Based NOMA for the Next Generations of Wireless Communications", *2022 International Conference on Electrical Engineering and Informatics (ICELTICs)*, Banda Aceh, Indonesia, 2022 (<https://doi.org/10.1109/ICELTICs56128.2022.9932105>).
- [11] M.F. Sohail, C.Y. Leow, and S. Won, "Non-orthogonal Multiple Access for Unmanned Aerial Vehicle Assisted Communication", *IEEE Access*, vol. 6, pp. 22716–22727, 2018 (<https://doi.org/10.1109/ACCESS.2018.2826650>).
- [12] X. Hu, C. Zhong, and Z. Zhang, "Angle-domain Intelligent Reflecting Surface Systems: Design and Analysis", *IEEE Transactions on Communications*, vol. 69, pp. 4202–4215, 2021 (<https://doi.org/10.1109/TCOMM.2021.3064328>).
- [13] N. Ben Halima, "Non Orthogonal Multiple Access (NOMA) Using a Nonlinear Energy Harvesting Model", *Wireless Personal Communications*, vol. 135, pp. 2165–2175, 2024 (<https://doi.org/10.1007/s11277-024-11129-9>).
- [14] M. Jain, S. Soni, N. Sharma, and D. Rawal, "Performance Analysis at Far and Near User in NOMA Based System in Presence of SIC Error", *AEU-International Journal of Electronics and Communications*, vol. 114, art. no. 152993, 2020 (<https://doi.org/10.1016/j.aeu.2019.152993>).
- [15] J.S. Roy, "Multiple-antenna Techniques in Wireless Communication Technical Aspects", *International Journal of Information Communication Technology and Digital Convergence*, vol. 1, pp. 24–32, 2016 (<https://doi.org/10.17577/IJERTCONV4IS01013>).
- [16] X. Luo, H. Li, Y. Bai, and S. Wei, "Research on Power Allocation Algorithm in Non-orthogonal Multiple Access Systems", 2019 14th IEEE Conference on Industrial Electronics and Applications (ICIEA), Xi'an, China, 2019 (<https://doi.org/10.1109/ICIEA.2019.8834152>).
- [17] A. Al-Hourani, S. Kandeepan, and A. Jamalipour, "Modeling Air-to-ground Path Loss for Low Altitude Platforms in Urban Environments", *2014 IEEE Global Communications Conference*, Austin, USA, 2014 (<https://doi.org/10.1109/GLOCOM.2014.7037248>).
- [18] A.A. Saeed and M.A. Ahmed, "Algorithms and Throughput Analysis of Cognitive Radio-based MIMO-NOMA for the Next Generation of Wireless Communications", *Transactions on Emerging Telecommunications Technologies*, vol. 35, art. no. e4988, 2024 (<https://doi.org/10.1002/ett.4988>).
- [19] J. Miranda *et al.*, "Path Loss Exponent Analysis in Wireless Sensor Networks: Experimental Evaluation", *2013 11th IEEE International Conference on Industrial Informatics (INDIN)*, Bochum, Germany, 2013 (<https://doi.org/10.1109/INDIN.2013.6622857>).
- [20] A. Doukas and G. Kalivas, "Rician K Factor Estimation for Wireless Communication Systems", *2006 International Conference on Wireless and Mobile Communications (ICWMC'06)*, Bucharest, Romania, 2006 (<https://doi.org/10.1109/ICWMC.2006.81>).
- [21] Z. Ding, Z. Yang, P. Fan, and H.V. Poor, "On the Performance of Non-orthogonal Multiple Access in 5G Systems with Randomly Deployed Users", *IEEE Signal Processing Letters*, vol. 21, pp. 1501–1505, 2014 (<https://doi.org/10.1109/LSP.2014.2343971>).
- [22] A.A. Saleh and M.A. Ahmed, "Performance Enhancement of Cooperative MIMO-NOMA Systems Over Sub-6 GHz and mmWave Bands", *Journal of Telecommunications and Information Technology*, no. 2, 2023 (<https://doi.org/10.26636/jtit.2023.170023>).
- [23] Z. Cui *et al.*, "Wideband Air-to-ground Channel Characterization for Multiple Propagation Environments", *IEEE Antennas and Wireless Propagation Letters*, vol. 19, pp. 1634–1638, 2020 (<https://doi.org/10.1109/LAWP.2020.3012889>).
- [24] R. Chandrasekhar *et al.*, "Performance Evaluation of MIMO-NOMA for the Next Generation Wireless Communications", *2021 3rd International Conference on Signal Processing and Communication (ICSPC)*, Coimbatore, India, 2021 (<https://doi.org/10.1109/ICSPC51351.2021.9451780>).
- [25] S. Li, X. Liu, J. Gaber, and G. Pan, "Modeling Analysis for Downlink RIS-UAV-assisted NOMA over Air-to-ground Line-of-sight Rician Channels", *Drones*, vol. 8, art. no. 659, 2024 (<https://doi.org/10.3390/drones8110659>).
- [26] M. Zeng *et al.*, "Capacity Comparison Between MIMO-NOMA and MIMO-OMA with Multiple Users in a Cluster", *IEEE Journal on Selected Areas in Communications*, vol. 35, pp. 2413–2424, 2017 (<https://doi.org/10.1109/JSAC.2017.2725879>).
- [27] A. Abd Saeed and M.A. Ahmed, "Cognitive Radio Based NOMA for the Next Generations of Wireless Communications", *2022 International Conference on Electrical Engineering and Informatics (ICELTICs)*, Banda Aceh, Indonesia, 2022 (<https://doi.org/10.1109/ICELTICs56128.2022.9932105>).

Ameer Y. Sadeeq, Student

College of Electronics Engineering

 <https://orcid.org/0009-0006-5514-541X>

E-mail: ameer.yaseen@stu.uoninevah.edu.iq

Ninevah University, Mosul, Iraq

<https://uoninevah.edu.iq>**Mohamad A. Ahmed, Ph.D.**

College of Electronics Engineering

 <https://orcid.org/0000-0001-6412-2275>

E-mail: mohamad.alhabbar@uoninevah.edu.iq

Ninevah University, Mosul, Iraq

<https://uoninevah.edu.iq>